Biogeochemistry (2014) 120:133–147
DOI 10.1007/s10533-014-9986-x

Biogeochemical regime shifts in coastal landscapes: the contrasting effects of saltwater incursion and agricultural pollution on greenhouse gas emissions from a freshwater wetland

Ashley M. Helton · Emily S. Bernhardt · Anna Fedders

Received: 31 October 2013 / Accepted: 14 April 2014 / Published online: 20 May 2014

Abstract Many coastal plain wetlands receive nutrient pollution from agricultural fields and are particularly vulnerable to saltwater incursion. Although wetlands are a major source of the greenhouse gases methane (CH_4) and nitrous oxide (N_2O), the consequences of salinization for greenhouse gas emissions from wetlands with high agricultural pollution loads is rarely considered. Here, we asked how saltwater exposure alters greenhouse gas emissions from a restored freshwater wetland that receives nutrient loading from upstream farms. During March to November 2012, we measured greenhouse gases along a ~2 km inundated portion of the wetland. Sampling locations spanned a wide chemical gradient from sites receiving seasonal fertilizer nitrogen and sulfate (SO_4^{2-}) loads to sites receiving seasonal increases in marine salts. Concentrations and fluxes of CH_4 were low (<100 μg L^{-1} and <10 mg m^{-2} h^{-1}) for all sites and sampling dates when SO_4^{2-} was high (>10 mg L^{-1}), regardless of whether the SO_4^{2-} source was agriculture or saltwater. Elevated CH_4 (as high as 1,500 μg L^{-1} and 45 mg m^{-2} h^{-1}) was only observed on dates when air temperatures were >27 °C and SO_4^{2-} was <10 mg L^{-1}. Despite elevated ammonium (NH_4^+) for saltwater exposed sites, concentrations of N_2O remained low (<5 μg L^{-1} and <10 μg m^{-2} h^{-1}), except when fertilizer derived nitrate (NO_3^-) concentrations were high and N_2O increased as high as 156 μg L^{-1}. Our results suggest that although both saltwater and agriculture derived SO_4^{2-} may suppress CH_4, increases in N_2O associated with fertilizer derived NO_3^- may offset that reduction in wetlands exposed to both agricultural runoff and saltwater incursion.

Keywords Methane · Nitrous oxide · Nitrate · Sulfate · Seawater intrusion · Restoration

Introduction

Many coastal plain wetlands receive large amounts of runoff from upstream urban and agricultural lands, and experience the leading edge of saltwater incursion, the landward movement of salinity from the ocean onto the coastal plain. Increased drought and hurricane intensity coupled with sea level rise (IPCC 2012) will likely increase the upstream extent of brackish water and peak salinities (Day et al. 2007; Anderson and Lockaby 2012) and substantially enhance nitrogen loading (Paerl et al. 2001) to widespread freshwater

Electronic supplementary material The online version of this article (doi:10.1007/s10533-014-9986-x) contains supplementary material, which is available to authorized users.

A. M. Helton (✉)
Department of Natural Resources and the Environment & the Center for Environmental Sciences and Engineering, University of Connecticut, Storrs, CT 06269, USA
e-mail: ashley.helton@uconn.edu

E. S. Bernhardt · A. Fedders
Department of Biology, Duke University, Durham, NC 27708, USA

coastal ecosystems. Because wetlands play a disproportionate role relative to the area they comprise in terms of nutrient transformation, water purification, and other ecosystem services (Costanza et al. 1997), restoration of marginal farmland is deployed as a strategy to protect sensitive coastal areas from nutrient loading (Zedler 2003) and may also buffer inland areas from sea level rise and storm surges (Costanza et al. 2008). Wetlands are also important global sources of greenhouse gases (Bloom et al. 2010; Nisbet et al. 2014), but greenhouse gas production is rarely considered during restoration activities (Morse et al. 2012; Brinson and Eckles 2011). With increasing sea level rise, the leading edge of saltwater incursion will move farther inland, inundating wetlands that already receive nutrient pollution or are recently restored farm fields. The resulting balance between wetland ecosystem services and greenhouse gas emissions will be important for understanding the future role of coastal plain wetlands in global biogeochemical cycles.

Saltwater incursion dramatically changes the chemistry of freshwater wetlands by introducing high salinity and high alkalinity waters rich in base cations and anions, including chloride (Cl^-) and sulfate (SO_4^{2-}). Such a chemical regime shift has great potential to alter microbial process rates, and resulting trace gas emissions. Thermodynamics would predict that saltwater incursion should reduce methane (CH_4) emissions from typically freshwater wetlands; SO_4^{2-} is a more efficient electron acceptor than carbon, and thus SO_4^{2-} reducers are expected to outcompete methanogens for limited fermentation products when supplied with large quantities of SO_4^{2-} (Megonigal and Hines 2003). The consequences of saltwater incursion for nitrous oxide (N_2O) emissions are more difficult to predict. An increase in hydrogen sulfide (H_2S) as a product of SO_4^{2-} reduction in saltwater exposed soils may prove particularly toxic to some nitrifiers, which oxidize ammonium (NH_4^+) to nitrate (NO_3^-) with N_2O gas as a byproduct, and denitrifiers, which reduce NO_3^- to N_2O and N_2 gases (Joye and Hollibaugh 1995; Senga et al. 2006). Alternatively, increases in H_2S have been shown to stimulate other denitrifying microbes capable of using H_2S as an electron donor (Brettar and Rheinheimer 1991; Burgin et al. 2012), with unknown consequences for both denitrification rates and for the N_2O yield (N_2O:N_2) of denitrification.

Contemporary patterns of agricultural drainage and historic patterns of agricultural land uses underlay the spatial patterns of saltwater incursion. Direct agricultural drainage increases nutrient concentrations and resulting eutrophication in receiving coastal plain wetlands (Smith et al. 2006). Much research has shown that elevated NO_3^- increases denitrification and subsequent N_2O emissions (Verhoeven et al. 2006). Denitrification is more energetically favorable, and should outcompete methanogenesis for fermentation products (Megonigal and Hines 2003), suppressing CH_4 emissions from wetlands that receive high NO_3^- loads from agriculture.

Marginally productive agricultural lands in former wetlands are often candidates for restoration (Heimlich et al. 1998; Zedler 2003). For example, in the southeastern USA, coastal plain wetlands were historically drained and filled for intensive row crop agriculture and consolidated feeding operations (Carter 1975; Dahl 1990; Barendregt et al. 2009). Restoration typically involves re-contouring fields to reduce drainage, removing barriers to water exchange, and planting wetland obligate woody plants (De Steven and Gramling 2012). These field-to-wetland restoration sites are particularly susceptible to saltwater incursion upon hydrologic reconnection to the sea because they have experienced a loss in soil elevation of up to 1 m (O'Driscoll 2012). Recent research demonstrates past inorganic fertilizer application increases the potential for export of legacy nutrients from these soils during re-flooding (Ardón et al. 2010) which can be further exacerbated by saltwater incursion, as marine salts extract sorbed NH_4^+ from wetland soils (Weston et al. 2010; Ardón et al. 2013). There is concern that these high NH_4^+ concentrations can exacerbate coastal nitrogen loading while also stimulating N_2O produced from nitrification or coupled nitrification–denitrification. Recent work in the coastal plain of North Carolina, USA saw no evidence of enhanced N_2O production from re-flooding (Morse et al. 2012), but we do not yet know how the added complication of saltwater incursion may alter the N_2O consequences of restoration.

In this study, we asked: How does saltwater incursion alter the concentrations and fluxes of CH_4 and N_2O from a restored freshwater coastal plain wetland receiving agricultural runoff? We predicted that CH_4 emissions would be low in areas receiving either saltwater or high agricultural runoff due to SO_4^{2-} reducers outcompeting methanogens in salty sites and denitrifiers outcompeting methanogens in sites exposed to farm runoff. We also predicted that

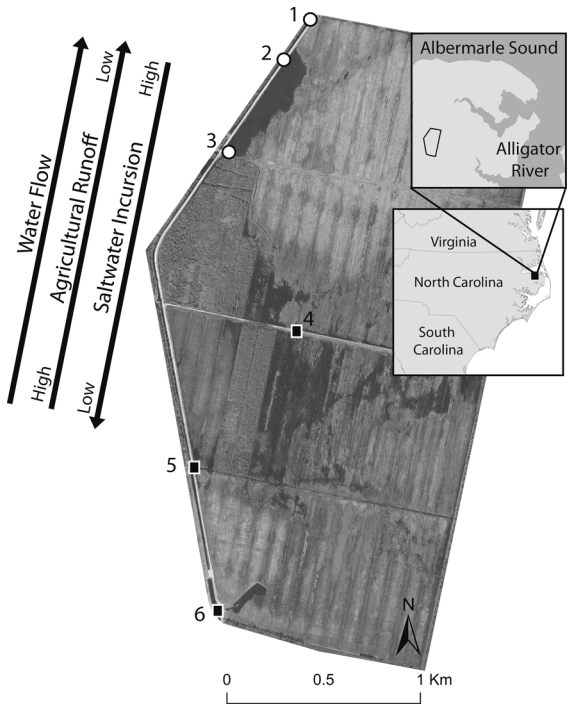

Fig. 1 Map of the site in relation to the coast of North Carolina (*insets*). Sampling locations (1–6) for sites that experienced saltwater incursion (*circles*) and agricultural runoff (*squares*) during 2012

elevated NH_4^+ and H_2S associated with saltwater incursion and elevated NH_4^+ and NO_3^- associated with agricultural runoff would increase N_2O emissions at both salty and nitrogen polluted sites via enhanced rates of nitrification, denitrification, coupled nitrification–denitrification and/or sulfur driven NO_3^- reduction. To test our predictions, we measured dissolved concentrations and fluxes of N_2O and CH_4 within a recently restored wetland that receives runoff from upstream agricultural fields and experiences seasonal saltwater incursion. We sampled trace gases and water chemistry for six permanently inundated sites that spanned the range of saltwater and agricultural runoff exposure of the wetland on 12 sampling dates that encompassed a seasonal saltwater incursion event and periods of fertilizer application to upstream fields.

Study site

Samples were collected from a 440 hectare restored wetland (Fig. 1) within the Timberlake Observatory for Wetland Restoration (TOWeR), a 1,700 hectare compensatory wetland mitigation site. TOWeR is located on the Albemarle Peninsula, in the Outer Coastal Plain of North Carolina, USA (Fig. 1, inset), and drains to the Little Alligator River, which flows into the Alligator River and the Albemarle Sound. The Albemarle Sound is a seasonally brackish microtidal system with wind-driven tides (Corbett et al. 2007).

Similar to most of the region, in the 1970s, large areas of swamp forests in TOWeR were cleared, drained, and converted to agriculture (Carter 1975). The former corn and soybean farmland within TOWeR is the restored wetland that is the focus of our study (Fig. 1). Restoration of the TOWeR agricultural area towards a forested wetland began in 2004 by lowering field crowns and filling drainage ditches and then planting 750,000 live saplings of obligate and facultative wetland tree species. In 2007, the former fields were hydrologically connected to both the upstream forest and downstream waters by disabling the downstream pump system, allowing the water table to rise and the site to be re-inundated by rain and wind tides. The site still receives pumped water from upstream agricultural fields (near site 6, Fig. 1) and receives upstream flow from a forested wetland area (site 5, Fig. 1). Flows at the site can move either upstream or downstream depending largely on rainfall and wind direction (Ardón et al. 2010), and the site is seasonally brackish with salinities peaking between 2 and 6 ppt near site 2 (Fig. 1) (Ardón et al. 2013). The region, site, and the restoration practices have been described in detail by Ardón et al. (2010) and Morse et al. (2012).

Methods

We sampled six sites on 12 sampling dates from March to November 2012 for water chemistry and dissolved CH_4 and N_2O, and in May, July, August, and October 2012 for CH_4 and N_2O flux from floating chambers. All sampling locations were permanently inundated (i.e., standing water >50 cm during all sampling events), and spanned the longitudinal extent of the restored wetland (Fig. 1). During 2012, sites 1, 2, and 3 experienced drought-induced saltwater incursion, with a peak salinity of 2.25 ppt occurring in late summer. Sites 4, 5, and 6 remained fresh during 2012, but received agricultural drainage pumped from upstream farm fields during two sampling events.

Dissolved gases

Water samples for measuring dissolved gas concentrations were collected in triplicate, and headspace equilibration techniques were used to extract gas samples for analysis (modified from Hudson 2004). We collected 80–100 ml of water in pre-weighed, crimp-capped, pre-evacuated 120-ml glass serum bottles by inserting a 20 gauge needle through the septum 2–5 cm below the water surface. Water samples were stored septum-side down, and headspace equilibrations were performed within 24 h. We injected N_2 gas to overpressurize the headspaces of bottles, and bottles were shaken for 2 min before a 10-ml headspace gas sample was extracted. For each sample, we measured temperature and pressure at the time of the equilibration, and calculated salinity (S) based on the empirical relationship between Cl^- concentration and S across the site (S (ppt) = 0.00167 Cl^- (ppm) + 0.0151; $r^2 = 0.99$). Water samples taken in conjunction with dissolved gas samples were analyzed for Cl^- concentrations (see Water sample collection and analyses, below). The precise volume of each water sample (V_w) and headspace (V_h) was determined by weighing each filled serum bottle on a Mettler Toledo PB precision balance (0.01 g).

To determine the concentration of dissolved gas in the original water sample, first we measured the dissolved gas concentrations extracted from the headspace after equilibration (see Gas analyses, below). Second, we calculated the aqueous concentration in the headspace after equilibration (C_{AH}) (i.e., the gas component that was originally in the liquid phase but was partitioned into the gas phase during the equilibration) (Hudson 2004):

$$C_{AH} = \frac{V_h}{V_w} \times C_g \times \rho_g \quad (1)$$

where C_g is the measured concentration of gas (g) converted to the decimal equivalent of the volumetric concentration (ml/ml), and ρ_g is the density of the gas (mg L^{-1}). Third, we calculated Henry's Law constants with equations provided by Fogg and Sangster (2003) for CH_4 and N_2O for each sample using measured temperature at the time of headspace extraction and salinity. Fourth, we used Henry's Law constants to calculate the aqueous concentration in water after equilibration (C_A) (i.e., the saturation concentration of the gas component, or the gas remaining in dissolved form after equilibration) (Hudson 2004):

$$C_A = \frac{n_w}{V_w} \times \frac{p_g}{H} \times MW_g \quad (2)$$

where $\frac{n_w}{V_w}$ is the molar concentration of water (55 mol L^{-1}), p_g is the partial pressure of the measured gas concentration (atm) ($p_g = C_g \times p_T$, where p_T is air pressure measured at the time of the equilibration), H is Henry's Law constant for the gas and sample (atm mol fraction^{-1}), and MW_g is the molecular weight of the gas (mg mol^{-1}). Finally, the concentration of gas in the original water sample was calculated as the sum of C_{AH} and C_A.

Gas fluxes

We applied the static chamber approach (Livingston and Hutchinson 1995) to measure water–atmosphere gas fluxes. We constructed floating chambers using 10 L gas sampling bags (Supelco Analytical, Tedlar Bags) cut open at one end and attached to square PVC pipe platforms. The gas bag was anchored with PVC pipe attached to the center of each side of the base, and a loop of fine gauge vinyl tubing was connected between the gas bag's push–pull lock valve and a gas tight 3-way valve (see Supplemental Fig. 1 for chamber design). At the time of sampling, the headspace in each chamber was mixed by flushing 15 times with a 60 mL syringe attached to a gas-tight 3-way valve before 10 mL gas samples were collected using a gas-tight glass syringe. Samples were collected immediately following chamber deployment and approx. 8 and 24 h post-deployment. Gas samples were collected in triplicate at each sampling interval and injected into 9-mL pre-evacuated glass vials (Teledyne Tekmar, Mason, OH, USA). Air temperature, barometric pressure, and water temperature were recorded with each gas sample collection.

Under ideal conditions, gases accumulate (or are consumed) linearly over time during static chamber incubations, and gas fluxes are calculated as the slope of the simple linear regression between concentration and time. We converted measured gas concentrations (ppmv; see Gas analyses, below) to μg m^{-3} using the ideal gas law and field measurements of barometric pressure and air temperature in R 2.13.0 (R Core Team 2012). From replicate determinations of gas samples, we calculated the minimum detectable concentration

(MDCD) difference for each sampling date (Yates et al. 2006; Matson et al. 2009). All gas fluxes were greater than the MDCD in this study, so we used the slope of concentration vs. time when $r^2 > 0.90$. When the accumulation rate was nonlinear, we used the rate during the first interval. Static chambers are sensitive to disturbance and chamber effects, and thus we excluded incubations with elevated initial concentrations and incubations in which the concentration increased significantly then decreased significantly, or vice versa.

To determine the volume of floating chambers, we performed laboratory sulfur hexafluoride (SF_6) injections into chambers deployed in 30 cm of tap water in large plastic bins. We diluted SF_6 with ambient air to 100 ppmv and injected 50 ml into each chamber with a syringe connected to the 3-way sampling valve. We mixed the SF_6 in the chamber by flushing 15 times with a 60 ml syringe. Gas samples were collected in triplicate 3 h after SF_6 injection and analyzed within 1 week of collection (see "Gas analyses" section). We calculated the volume of each floating chamber (V_{FC}):

$$V_{FC} = \frac{V_{INJ} C_{INJ}}{C_{FC}} \quad (3)$$

where V_{INJ} is the volume of SF_6 injected into the chamber (i.e., 50 ml), C_{INJ} is the concentration of SF_6 injected into the chamber (100 ppmv), and C_{FC} is the average concentration measured from the sample collected from the chamber. We also directly measured the surface area of the water enclosed by the chamber. Trace gas fluxes calculated from field incubations were multiplied by the chamber volume and divided by the surface area derived from SF_6 laboratory injections to report flux rates per unit area of water surface.

Gas analyses

Gas samples were analyzed within 2 weeks of collection as described in detail by Morse et al. (2012). Briefly, gas samples were analyzed for N_2O and CH_4 (and SF_6 for laboratory tests, see Gas fluxes, above) concentrations injected by a Tekmar 7050 Headspace Autosampler to a Shimadzu 17A gas chromatograph with electron capture detector (ECD) and flame ionization detector (FID; Shimadzu Scientific Instruments, Columbia, MD, USA), retrofitted with sixport valves and a methanizer to allow the determination of the gas concentrations from the same sample. Ultra-high purity N_2 was used as the carrier gas, and a P5 mixture served as the make-up gas for the ECD. A Nafion tube (Perma Pure, Toms River, NJ, USA) and counter-current medical breathing air were used to remove water vapor from the sample stream. Gas concentrations were determined by comparing to peak areas of samples and known standards (certified primary standards; Airgas, Morrisville, NC, USA), and calculated as the average of two of three replicate samples. If the relative percent difference of the samples exceeded 10 %, then the third replicate was analyzed and the average of the higher two replicates was retained, since we assume most sampling error is associated with syringe or vial leaks or inadvertent capture of ambient air during sampling.

Water sample collection and analyses

Water samples were collected in conjunction with dissolved gas samples. Each water sample was collected by 60 mL syringe and filtered immediately upon collection through 0.7 μm GF/F Whatman filters in syringe–filter holders. Filtered samples were collected in acid washed and field rinsed bottles, transported to the lab on ice, and frozen until analysis.

Water samples were analyzed according to standard methods (APHA 1998). Soluble reactive phosphorus (SRP; ascorbic acid method) and NH_4^+ (phenate method) were analyzed on a Lachat QuikChem 8000 (Lachat Instruments, Milwaukee WI, USA). Minimum detection limits were 5 μg N L^{-1} for NH_4^+ and 2.5 μg L^{-1} for SRP. We measured NO_3^-, Cl^- and SO_4^{2-} on a Dionex ICS-2000 ion chromatograph (Dionex Corporation, Sunnyvale, CA, USA). Minimum detection limits were 5 μg N L^{-1} for NO_3^-, 0.03 mg L^{-1} for Cl^-, and 0.01 mg L^{-1} for SO_4^{2-}. Total dissolved nitrogen (TDN) and dissolved organic carbon (DOC) were measured on a Shimadzu TOC-V total carbon analyzer with a TNM-1 nitrogen module (Shimadzu Scientific Instruments, Columbia, MD, USA). Minimum detection limits were 0.25 mg L^{-1} for DOC and 0.05 mg L^{-1} for TDN. Concentrations measured below detection were set to one half the detection limits. We calculated dissolved inorganic nitrogen (DIN) as the sum of NO_3^- and NH_4^+ concentrations. Water pH, conductivity, and temperature were measured when we collected samples using a handheld meter (Beckman Coulter model pHi 470).

We also measured H_2S concentrations by the methylene blue spectrophotometric method (Golterman and Clymo 1969) during the August and September sampling events, adding reagents immediately in the field. Samples were kept in the dark and read at 663 nm on a LKB Biochrom Ultraspec II spectrophotometer (Biochrom, Holliston, MA, USA) within 1 week of collection. Standards were prepared with sodium sulfide ($Na_2S{\cdot}9H_20$).

Statistical analyses

Statistical analyses were performed in R 2.13.0 (R Core Team 2012). To visualize water chemistry and trace gas datasets, we used chull() to outline the convex hull of selected scatter plots. A convex hull is the smallest convex polygon in a plane that contains all of the points of a given dataset. We performed single factor repeated measures analyses of variance with Anova() in the CAR package and post hoc Tukey HSD comparison to test for differences between sites for water chemistry and dissolved trace gases. We performed simple linear regressions between trace gas concentrations and water chemistry parameters for individual dates with lm(). For the full dataset, we performed multiple linear regression model selection for dissolved gases using regsubsets() in the LEAPS package. Dependent variables included dissolved solute concentrations (DOC, NO_3^-, NH_4^+, SO_4^{2-}, Cl^-), pH, and air temperature. We did not include SRP because it was typically below detection, water temperature because it was strongly correlated with air temperature ($r^2 = 0.62$), and conductivity because it was strongly correlated with Cl^- ($r^2 = 0.99$). Variables were Ln() transformed to meet test assumptions as needed. We also converted CH_4 and N_2O concentrations and fluxes to CO_2 equivalents by multiplying CH_4 by 25 and N_2O by 298, based on the IPCC's 100-year time horizon estimates (Forster et al. 2007).

Results

Water chemistry

The concentrations of major ions varied in both time and space across the sampling transect (Fig. 2; Table 1). Late summer saltwater incursion increased Cl^- concentrations in saltwater exposed sites by two orders of magnitude (35 to a maximum of 1,337 mg L^{-1}) while Cl^- in sites 4, 5 and 6 remained below 60 mg L^{-1} (Fig. 2a). As expected, elevated salinity in saltwater exposed sites was associated with concomitant increases in pH (pH 4–7; Fig. 3a). The site nearest the agricultural fields (site 6) also experienced equivalent increases in pH (Figs. 2b, 3b), presumably as a result of agricultural chemicals.

Concentrations of SO_4^{2-} in surface waters tracked pH rather than salinity. As expected, saltwater exposed sites showed a wide range of SO_4^{2-} concentrations (Fig. 3c) increasing from a background of $\sim$1 mg L^{-1} to a maximum of 150 mg L^{-1} during summer saltwater incursion (Fig. 2c). Concentrations of SO_4^{2-} for the site nearest the farm fields were also elevated, and remained elevated during all sampling dates, ranging from 10 to 42 mg SO_4^{2-} L^{-1} (Figs. 2c, 3d). Ammonium concentrations followed a similar pattern (Table 1), with higher NH_4^+ concentrations at saltwater exposed sites (maximum at 0.48 mg N L^{-1}) and the site nearest the agricultural fields (maximum at 0.85 mg N L^{-1}) than the interior wetland sites, which remained below 0.11 mg N L^{-1} (Fig. 2d).

In contrast to SO_4, NH_4 and pH, concentrations of DIN were unaffected by saltwater incursion, typically remaining below 0.5 mg N L^{-1} for saltwater exposed sites (Fig. 3c). Higher DIN concentrations (>1 mg N L^{-1}) for sites exposed to agricultural runoff were driven by high NO_3^- concentrations at the site nearest the farm fields in the spring and at the three sites nearest the farm fields (sites 4, 5, and 6) during the fall (Fig. 2e). DOC concentrations did not appear to follow saltwater incursion or agricultural runoff gradients. DOC concentrations ranged from 18 to 50 mg L^{-1} across the wetland and were lowest in the most upstream site that drains the agricultural field (site 6), highest for the site that drains a large forested wetland (site 5), and intermediate for sites nearest the saltwater incursion source (sites 1 and 2) (Table 1; Fig. 2f). Hydrogen sulfide was below detection for all surface water samples collected during August and September.

Greenhouse gases

Greenhouse gas concentrations and fluxes also varied across the site with saltwater incursion and agricultural runoff, with a lower range of both CH_4 and N_2O

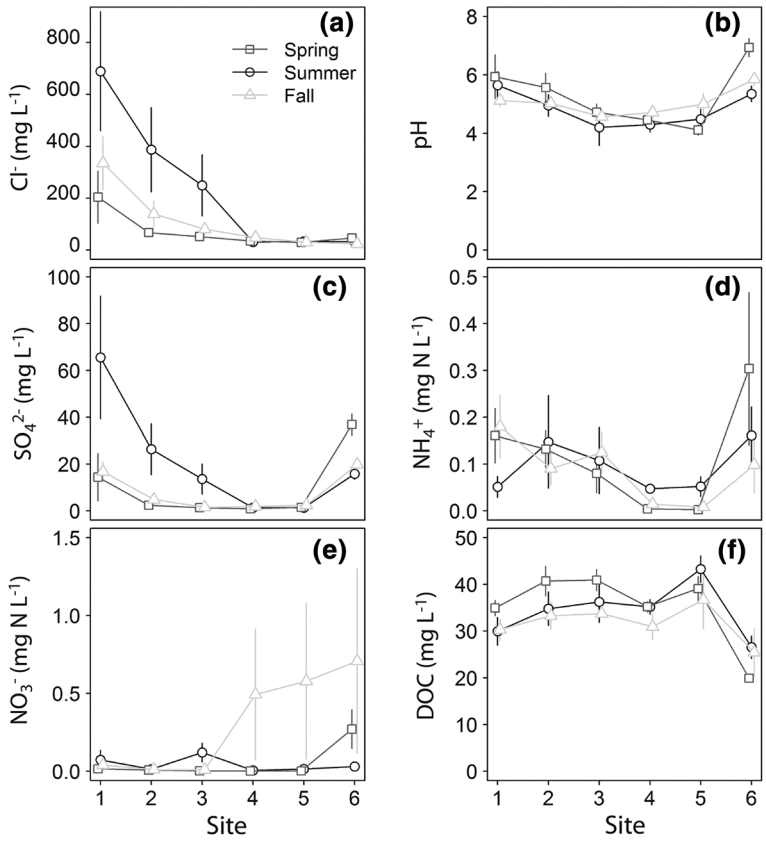

Fig. 2 Concentrations of **a** Cl^-, **b** pH, **c** SO_4^{2-}, **d**NH_4^+, **e** NO_3^-, and **f** DOC by season (mean ± std. error) for each sampling site (locations in Fig. 1). Single-factor repeated measures ANOVA results reported in Table 1

for saltwater exposed sites (Fig. 3e–f). Concentrations and fluxes of CH_4 were lower in saltwater exposed sites (Table 1), particularly in summer months when interior wetland sites peaked as high as 1,500 μg L^{-1} and 45 mg m^{-2} h^{-1} but saltwater exposed sites remained below 350 μg L^{-1} and 10 mg $m^{-2}h^{-1}$ (Fig. 4a–b). Concentrations and fluxes of CH_4 were also low (<100 μg L^{-1} and <8 mg m^{-2} h^{-1}) at the site nearest the farm fields (Table 1; Fig. 4a–b), even during summer months when NO_3^- concentrations were low, but SO_4^{2-} concentrations remained elevated (Fig. 3).

Concentrations of CH_4 and SO_4^{2-} were strongly correlated for sampling dates during the peak of saltwater incursion (July–September; Table 2). Concentrations of CH_4 were not strongly or consistently related to other ion concentrations; they were not directly related to Cl^- on any individual sampling date ($p > 0.05$), and correlated to NO_3^- ($r^2 = 0.51$) and to DOC ($r^2 = 0.58$) concentrations for only one sampling date in September ($p < 0.05$). Multiple regression model selection also supports SO_4^{2-} as a strong driver of CH_4 patterns; SO_4^{2-} concentration was selected in best models for all parameter levels (Table 2). Concentrations of SO_4^{2-} alone explained 23 % of variation in dissolved CH_4 concentrations and 28 % of variation in CH_4 flux for the whole dataset (data Ln transformed for regression; $p < 0.05$) (Fig. 5). In fact, CH_4 concentrations and fluxes only exceeded 100 μg L^{-1} and 10 mg m^{-2} h^{-1} when SO_4^{2-} concentrations were lower than 10 mg L^{-1} (Fig. 5).

Dissolved N_2O concentrations and fluxes were uniformly low across the site (<5 μg L^{-1} and <10 μg m^{-2} h^{-1}), except during two spring and one fall sampling event when high concentrations of NO_3^- with correspondingly high concentrations of N_2O were measured at the agricultural runoff exposed sites (7–156 μg L^{-1}) (Fig. 4c). N_2O concentrations were significantly related to NO_3^- concentrations for individual dates when NO_3^- concentrations were high in the sites nearest the farm fields—in the early spring (March and April) and in the late fall (November) (Table 2). N_2O concentrations were also significantly

Table 1 Mean (std. dev.) of water chemistry and greenhouse gas concentrations, and single factor repeated measures ANOVA results (F statistic and p-value)

Parameter	Site						ANOVA
	1	2	3	4	5	6	F, p
Cl^- (mg L^{-1})*	555.11^{a} (492.47)	276.53^{b} (309.88)	171.95^{b} (189.75)	38.14^{c} (18.67)	31.16^{c} (7.84)	34.58^{c} (10.93)	30.50, <0.001
SO_4^{2-} (mg L^{-1})*	48.81^{a} (54.23)	18.43^{ab} (25.09)	8.71^{bc} (11.61)	1.30^{c} (1.16)	1.54^{c} (1.55)	22.63^{a} (11.78)	17.99, <0.001
NO_3^{-1} (µg N L^{-1})*	58.58^{a} (152.30)	12.34^{a} (12.80)	56.38^{a} (117.63)	117.49^{a} (404.97)	140.48^{a} (477.85)	261.97^{b} (573.92)	3.30, 0.01
NH_4^{+1} (µg N L^{-1})*	116.03^{a} (113.96)	114.62^{a} (127.83)	99.10^{a} (103.29)	27.65^{b} (28.78)	37.52^{b} (61.72)	220.03^{a} (224.81)	6.50, <0.001
TDN (mg L^{-1})*	1.32^{ab} (0.43)	1.42^{b} (0.47)	1.34^{b} (0.27)	1.16^{ab} (0.36)	1.57^{b} (0.86)	1.30^{a} (0.83)	3.86, 0.005
DOC (mg L^{-1})	31.24^{a} (5.62)	37.29^{a} (7.44)	36.82^{ab} (6.35)	33.93^{ab} (3.65)	40.00^{b} (7.42)	24.86^{c} (6.46)	26.38, <0.001
SRP (µg L^{-1})*	4.49 (2.49)	4.36 (1.97)	6.92 (3.31)	4.67 (2.31)	7.33 (7.00)	7.92 (8.50)	ns
pH	5.67^{ab} (0.92)	5.07^{b} (1.06)	4.37^{c} (0.74)	4.43^{c} (0.60)	4.59^{c} (0.65)	5.92^{a} (0.88)	17.27, <0.001
Diss. CH_4 (µg L^{-1})*	108.50^{a} (268.21)	50.86^{a} (120.05)	334.74^{bc} (533.03)	596.57^{c} (495.72)	344.67^{b} (583.85)	44.31^{a} (40.12)	9.73, <0.001
Diss. N_2O (µg L^{-1})**	0.28 (0.22)	0.73 (1.63)	0.28 (0.55)	1.04 (2.11)	1.74 (4.21)	12.94 (42.58)	ns

Letters denote significance from post hoc Tukey HSD. *Site 1* The most downstream site nearest the saltwater source. *Site 6* The most upstream site nearest the agricultural fields. See Fig. 1 for site locations and Figs. 2 and 4 for temporal trends

* Data were Ln transformed before analyses

** Diss. N_2O concentrations were transformed as Ln (N_2O + 1)

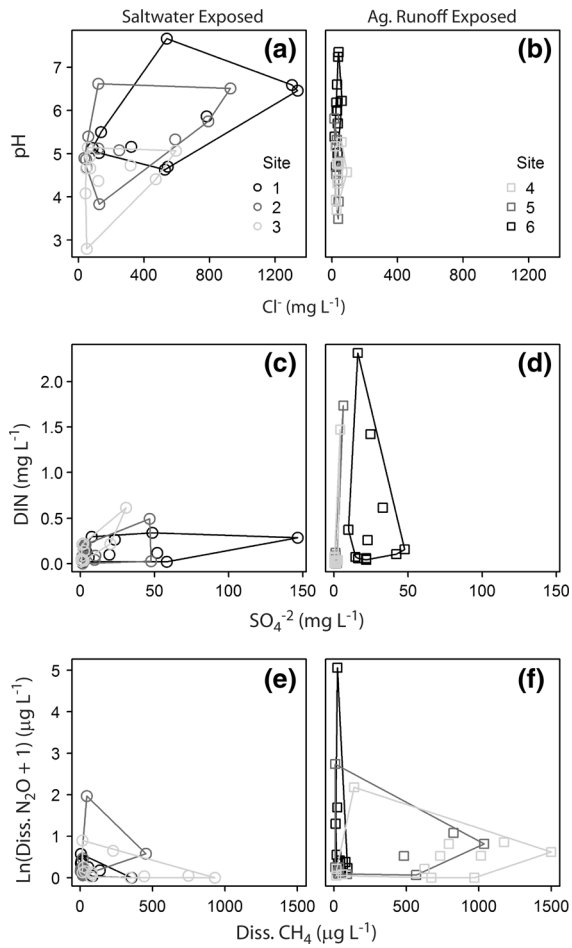

Fig. 3 Convex hull plots for **a**, **b** pH versus Cl^- concentrations, **c**, **d** NO_3^- versus SO_4^{2-} concentrations, and **e**, **f** dissolved N_2O versus CH_4 concentrations for sites that experienced saltwater incursion (**a**, **c**, and **e**) and sites that received agricultural runoff (**b**, **d**, **f**)

related to SO_4^{2-} (March: $r^2 = 0.96$, April: $r^2 = 0.99$) and DOC (March: $r^2 = 0.99$, April: $r^2 = 0.89$) concentrations during the two early spring sampling events ($p < 0.05$); NO_3^- concentrations during these two sampling events, which preceded saltwater incursion, were strongly correlated to DOC (March: $r^2 = 0.93$, April: $r^2 = 0.99$, $p < 0.05$) and SO_4^{2-} (March: $r^2 = 0.99$, April: $r^2 = 0.96$, $p < 0.05$). Dissolved N_2O concentrations were not correlated to DOC or SO_4^{2-} for any other individual dates ($p > 0.05$), and, despite elevated NH_4^+ concentrations in saltwater exposed sites (Table 1), were not correlated to NH_4^+ concentration for any individual dates ($p > 0.05$).

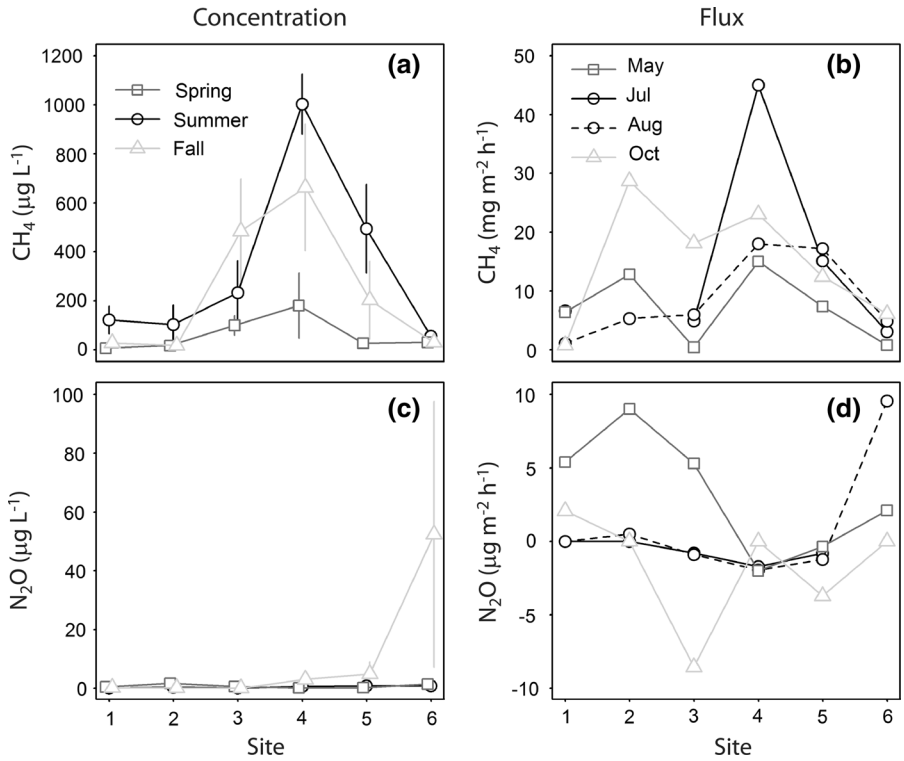

Fig. 4 Concentrations of **a** CH_4 and **c** N_2O and fluxes of **b** CH_4 and **d** N_2O for each site (locations in Fig. 1). Concentrations reported by season as mean ± std. error. Flux reported for each date gas flux was measured

Table 2 Simple linear regressions between dissolved CH_4 and SO_4^{2-} concentrations and between dissolved N_2O and NO_3^- concentrations for individual sampling events (n = 6 for each date)

Date	Model	
	$Ln(CH_4) \sim Ln(SO_4^{2-})$	$Ln(N_2O + 1) \sim Ln(NO_3^-)$
2 Mar 2012	ns	1.58, 0.224 ($r^2 = 0.84$)
3 Apr 2012	ns	0.619, 0.082 ($r^2 = 0.94$)
1 May 2012	ns	ns
22 May 2012	ns	ns
14 Jun 2012	ns	ns
3 Jul 2012	ns	ns
25 Jul 2012	6.33, −0.76 ($r^2 = 0.57$)	ns
7 Aug 2012	6.59, −0.62 ($r^2 = 43$)	ns
27 Aug 2012	5.53, −0.76 ($r^2 = 0.92$)	ns
17 Sep 2012	5.95, −0.95 ($r^2 = 77$)	ns
3 Oct 2012	ns	ns
1 Nov 2012	ns	2.96, 0.664 ($r^2 = 0.78$)

Regressions reported as intercept, slope when $p < 0.05$. ns denotes non-significant regressions

Multiple regression model selection also supports NO_3^- as the dominant driver of N_2O patterns; NO_3^- concentration was selected in best models for all parameter levels (Table 2), and NO_3^- concentration alone explained 37 % of variation in dissolved N_2O concentrations for the whole dataset (Table 3; Fig. 6a). Significant regression coefficients for SO_4^{2-} and Cl^- suggest that saltwater and SO_4^{2-} loading may also affect N_2O concentrations to some degree. Again, despite elevated NH_4^+ concentrations

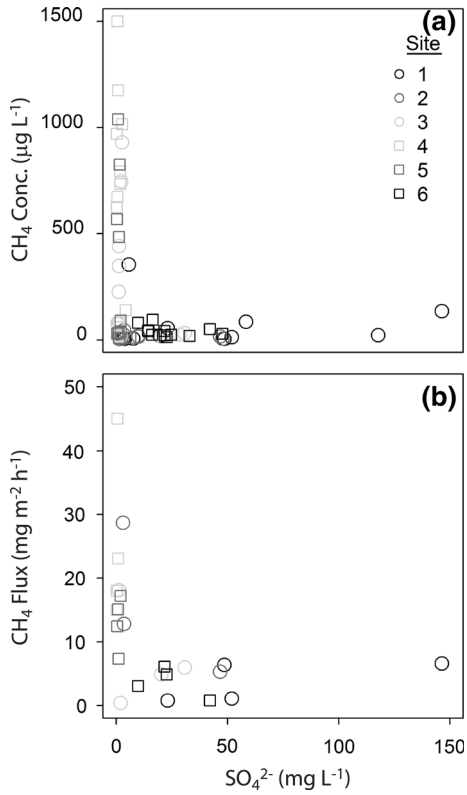

Fig. 5 **a** Dissolved CH_4 concentration and **b** CH_4 flux versus SO_4^{2-} concentration

in saltwater and agricultural runoff exposed sites, NH_4^+ concentration was not a significant variable in any models. Fluxes of N_2O were measured only in summer and early fall, and thus we did not capture flux rates corresponding to high NO_3^- concentrations in early spring and late fall (Fig. 4d). For the full dataset, N_2O fluxes were not correlated to NO_3^- (Fig. 6b) and weakly positively correlated to SO_4^{2-} ($r^2 = 0.13$) concentrations ($p < 0.10$).

Because our gas flux sampling events did not encompass periods of fertilizer runoff, we used dissolved gas concentrations converted to CO_2 equivalents to compare how saltwater incursion relative to agricultural runoff might change the contribution to radiative forcing from the restored wetland. CH_4 was the most important component for unexposed samples (Fig. 7). Saltwater incursion and agricultural runoff decreased the contribution of CH_4 by 7- and 15-fold, respectively; whereas agricultural runoff increased the contribution of N_2O by 60-fold. In terms of total CO_2 equivalents, saltwater exposure suppressed the overall radiative balance relative to unexposed sites. Although agricultural runoff altered the relative contribution of CH_4 and N_2O, it did not change the overall magnitude relative to unexposed sites.

Discussion

Coastal plain wetlands, situated between agricultural fields and coastal oceans, represent a particularly dynamic biogeochemical landscape. The simultaneous eutrophication from terrestrial runoff and salinization from saltwater incursion generate broad chemical gradients in both space and time that can be usefully employed to test our basic understanding of biogeochemical processes. Our results suggest that SO_4^{2-} loading (with or without accompanying increases in salinity) is likely to suppress coastal wetland CH_4 emissions, while SO_4^{2-} concentrations (at least within the range studied here) appear to have little effect on N_2O emissions. Instead, N_2O emissions appeared to be primarily controlled by NO_3^- supply from upstream farmlands in these permanently flooded (and DOC rich) wetlands. Our results suggest that reduction in CH_4 emissions via saltwater incursion may be offset by increases in N_2O emissions with increased agricultural runoff and inundation of former farm fields. We interpret these findings as encouraging early evidence that, despite the enormous chemical shifts experienced by these dynamic coastal landscapes, it may be possible to generate fairly simple predictions about the consequences for greenhouse gas emissions. To facilitate such predictions, future research must address (1) how greenhouse gas emissions respond to increasing intensity and duration of saltwater incursion, and (2) the timing and spatial juxtaposition of agricultural runoff and saltwater incursion within the coastal plain landscape, both of which we discuss below.

Response to changing intensity

Our results that elevated SO_4^{2-} suppress CH_4 emissions supports prior research; reductions in atmospheric SO_4^{2-} pollution increases wetland CH_4 emissions (Gauci et al. 2004), and CH_4 emissions from salt marshes are generally lower than from freshwater wetlands (Bartlett et al. 1987; Capone and Kiene 1988; Poffenbarger et al. 2011; Neubauer

Table 3 Candidate multiple regression models for dissolved CH_4 and N_2O concentrations for each possible number of model coefficients (K), including the intercept

Model	K	adj. r^2	C_p	AIC	Δ_i	RSS
Dissolved CH_4 Conc.						
SO_4^{2-}	2	0.23	14.51	44.77	11.51	115.98
SO_4^{2-}, Air Temp.	3	0.33	6.91	38.05	4.79	99.25
SO_4^{2-}, Air Temp., NO_3^-	4	0.38	3.75	34.73	1.47	90.23
SO_4^{2-}, Air Temp., NO_3^-, DOC	**5**	**0.41**	**2.64**	**33.26**	0	84.83
SO_4^{2-}, Air Temp., NO_3^-, DOC, pH	6	0.40	4.33	34.9	1.64	84.29
SO_4^{2-}, Air Temp., NO_3^-, DOC, pH, NH_4^+	7	0.39	6.10	36.63	3.37	83.88
SO_4^{2-}, Air Temp., NO_3^-, DOC, pH, NH_4^+, Cl^-	8	0.38	8.00	38.51	5.25	83.71
Dissolved N_2O Conc.						
NO_3^-	2	0.37	25.15	−43.83	17.39	23.84
NO_3^-, Cl^-	3	0.47	13.19	−53.01	8.21	19.52
NO_3^-, Cl^-, DOC	4	0.52	8.24	−57.53	3.69	17.38
NO_3^-, Cl^-, DOC, Air Temp.	5	0.55	5.86	−60.07	1.15	16.02
NO_3^-, Cl^-, DOC, Air Temp., SO_4^{2-}	**6**	**0.57**	**5.02**	**−61.22**	0	15.15
NO_3^-, Cl^-, DOC, Air Temp., SO_4^{2-}, pH	7	0.56	6.20	−60.17	1.05	14.89
NO_3^-, Cl^-, DOC, Air Temp., SO_4^{2-}, pH, NH_4^+	8	0.56	8.00	−58.41	2.81	14.83

Reported statistics include adjusted r^2 (r^2_{adj}), Akaike's Information Criterion (AIC), the difference between the candidate and best model's AIC (Δ_i), and the residual sum of squares (RSS). Data were transformed before analyses according to Table 1. Candidate models with lowest AIC are in bold and coefficients are reported in Table 4

Table 4 Multiple linear regression coefficient estimates (std. error) for model with lowest AIC (Table 3) for dissolved CH_4 and N_2O concentrations

Model	Diss. CH_4	Diss. N_2O
Intercept	3.95 (1.25)*	2.21 (0.536)*
Cl^-		−0.265 (0.087)*
SO_4^{2-}	−0.802 (0.147)*	0.135 (0.079)*
NH_4^+		
NO_3^-	0.226 (0.111)*	0.270 (0.048)*
DOC	−0.050 (0.028)*	0.041 (0.012)*
pH		
Air Temp.	0.149 (0.037)*	−0.036 (0.016)*
N	56	56
P	<0.0001	<0.0001

Data were transformed before analyses according to Table 1. * $p < 0.05$

2012). These patterns conform to the thermodynamic prediction that SO_4^{2-} reducers will outcompete methanogens for fermentation products when SO_4^{2-} concentrations are high (Megonigal and Hines 2003). Although some lab studies have found the counterintuitive result that saltwater exposure enhances CH_4 emissions from sediments (Weston et al. 2011), our field studies fall directly in line with thermodynamic predictions. Our results lead us to speculate that the threshold at which SO_4^{2-} suppresses CH_4 emissions in these ecosystems is quite low (10 mg L^{-1}), similar to the relationships observed between CH_4 suppression and SO_4^{2-} deposition in peatlands (Gauci et al. 2004) and sea salt-amendments to tidal forest soils in the laboratory (Marton et al. 2012). If true, the future trajectory for CH_4 emissions in these coastal wetlands is fairly certain. As sea level rise converts many coastal plain wetlands toward the SO_4^{2-} concentration of seawater (2700 mg L^{-1}), CH_4 may continue to be substantially suppressed (e.g., by ~85 % as observed in this study).

However, the magnitude of saltwater exposure in this study and in most laboratory studies is quite low relative to future trajectories for saltwater incursion (e.g., max. 2.25 ppt salinity and 150 mg L^{-1} SO_4^{2-} observed in current study relative to 35 ppt salinity and 2,700 mg L^{-1} of seawater), and the effects of salinity and SO_4^{2-} on CH_4 emissions may change with increasing saltwater concentrations. For example, salinity and SO_4^{2-} may differentially affect methanogens and methanotrophs, microbes that oxidize CH_4. There is some evidence that methanotrophs are more

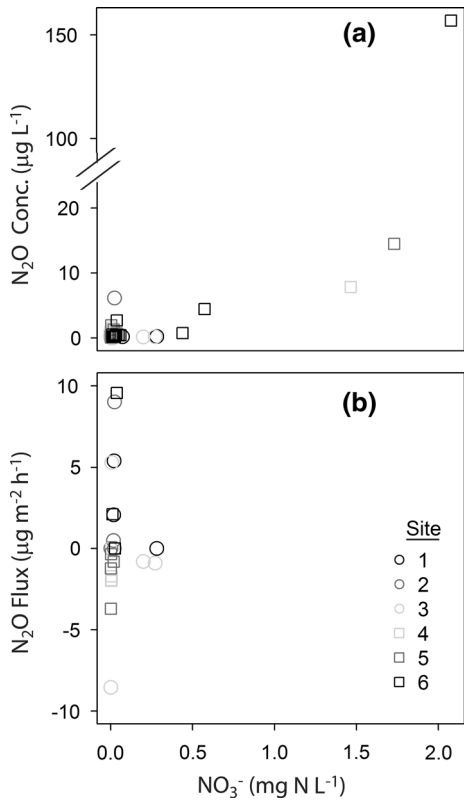

Fig. 6 **a** Dissolved N_2O concentration and **b** N_2O flux versus NO_3^- concentration

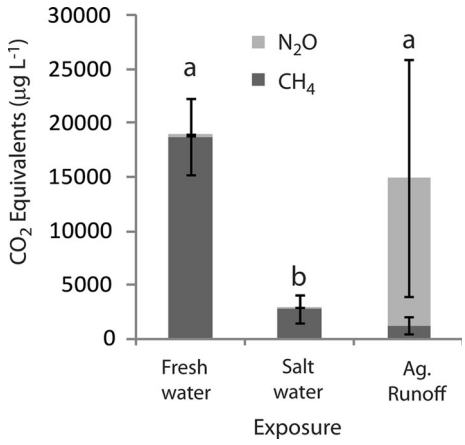

Fig. 7 CO_2 equivalents (mean ± std. error) for samples unexposed to saltwater or agricultural runoff (i.e., fresh water) (sites 4 and 5 during summer sampling dates; n = 10), samples exposed to saltwater (sites 1 and 2 during saltwater incursion; n = 10), and samples exposed to agricultural runoff (site 6 during spring and fall and sites 4 and 5 during fall; n = 5)

sensitive to salinity than are methanogens, with the potential for differential salinity tolerance to generate significant increases in net CH_4 fluxes at ecosystem scales (Conrad 1995; Segers 1998). Increased salinity with saltwater incursion also decreases the solubility of gases in water (Fogg and Sangster 2003); thus, a larger proportion of trace gases overall should escape solution when the water becomes saltier, regardless of microbial process rates. Sustained exposure to saltwater kills many salt-intolerant woody plants (Kozlowski 1997), which may also increase CH_4 emissions as plant material decomposes. Thus, there may be many alternate mechanisms driving CH_4 emissions for elevated salinities outside of the range of the current study, but likely to occur under future conditions.

High concentrations of N_2O occurred only when NO_3^- concentrations in surface waters were high. This pattern is entirely consistent with previous estimates of N_2O from periodically flooded (rather than permanently inundated) sections of our study site (Morse et al. 2012), and likely indicates a direct denitrifier response to fertilizer runoff. Although high N_2O concentrations were primarily associated with agricultural runoff, multiple regression analyses also suggest that incorporating variation in Cl^-, DOC and SO_4^{2-} further improved our predictions of N_2O concentration. Concentrations of N_2O were negatively related to Cl^-, suggesting saltwater exposure may inhibit microbial processes that produce or consume N_2O. This hypothesis is supported by previous research showing that Cl^- inhibits nitrification and denitrification, even at low Cl^-concentrations (Roseberg et al. 1986; Seo et al. 2008). Conversely, N_2O concentrations were positively related to SO_4^{2-} concentrations. It is certainly possible that these two anions could be having opposing effects on denitrifiers, as denitrifiers capable of using H_2S as an electron donor may be stimulated with increased SO_4^{2-} loads (Brettar and Rheinheimer 1991; Burgin et al. 2012). Although H_2S was below detection in surface water during this study, we have detected H_2S in porewater on the site (Hopfensperger et al. 2014) and during laboratory slurries of TOWeR soils (Helton unpublished data). These competing mechanisms may play a larger role as the intensity of saltwater incursion in coastal plain wetlands increases, with unknown consequences for net N_2O emissions.

On our site, agricultural runoff and saltwater exposure were segregated in space (sites 1–3 experienced saltwater exposure and sites 4–6 experienced

agricultural runoff) and time (saltwater incursion occurred during the summer whereas agricultural runoff occurred during the spring and fall). As climate change intensifies, these two chemical fronts will likely overlap more frequently in both space and time. The relatively straightforward relationship between NO_3^- and N_2O may change when fertilizer derived NO_3^- is added directly to sites with high salinity. Salinity and H_2S toxicity may suppress denitrification (Seo et al. 2008); conversely, sulfur-driven NO_3^- reduction may be stimulated (Burgin et al. 2012), with unknown consequences for the N_2O:N_2 yield of denitrification. The direction of this response will affect the likelihood of N_2O emissions offsetting the SO_4^{2-} induced reductions in CH_4 emissions likely to occur with saltwater incursion. Understanding the microbial response to these intersecting chemical fronts will be important for predicting the balance between greenhouse gas emissions and ecosystem services from coastal wetlands under future conditions.

Predicting novel chemical regimes

As climate change alters the intensity and timing of terrestrial runoff and the intensity, frequency, and extent of saltwater incursion, the chemical landscape of coastal plain wetlands will change dramatically. At the downstream boundary of coastal plain wetlands ecosystems, the spatial extent and intensity of saltwater incursion, which introduces high salinity and high alkalinity waters rich in base cations as well as Cl^- and SO_4^{2-}, will continue to expand. At the upstream boundary, coastal wetlands that already receive large amounts of agricultural runoff, which contains a complex mixture of chemicals, including fertilizers, lime, pesticides, and herbicides, may experience changes in timing and intensity of runoff from farm fields. Research describing agricultural runoff to aquatic systems has focused primarily on nutrient pollution and subsequent eutrophication in downstream aquatic systems (Smith et al. 2006). Increases in alkalinity (Oh and Raymond 2006) and SO_4^{2-} loading (Hyer et al. 2001; Collins and Jenkins 1996) have received less attention in recent literature, but also substantially alter the chemical composition of agricultural runoff to receiving wetlands.

Further complicating the biogeochemical landscape, converting marginal agricultural fields to restored wetlands is becoming increasingly common in the southeastern USA, and historic agricultural land uses will alter the geochemical response of wetlands to saltwater exposure. Inundation of previously flooded farm fields at the TOWeR study site has increased legacy nutrient export (Ardón et al. 2010). Saltwater incursion exacerbates legacy nutrient export since cations in seasalts can replace soil bound NH_4^+, increasing dissolved NH_4^+ in pore and surface water (Weston et al. 2010; Ardón et al. 2013). Indeed, restored wetlands with previous agricultural use at the TOWeR study site release significantly more soil bound nitrogen that natural wetlands (Ardón et al. 2013).

The hydrologic landscape of the southeastern USA coastal plain also plays a particularly important role in understanding the future chemical landscape. Extensive drainage networks and high volume pumps that actively drain farm fields act to reduce the hydrologic connectivity of wetlands to coastal waters, and thus moderate wetland exposure to marine salts. Recently, many marginal agricultural fields have been abandoned, placed in conservation easements, and/or actively restored to wetlands, in part by removing hydrologic barriers to natural water regimes. While restoring hydrology is important for restoring wetland ecosystems, it also increases the susceptibility of these systems to saltwater incursion. Thus, predicting the chemical regimes of coastal wetlands under future scenarios requires understanding not only current and historic chemical loadings, but also the extensive human modifications to the landscape's hydrologic network.

Conclusions

Our results suggest that both short-term, low intensity saltwater incursion events and SO_4^{2-} loading from agricultural fields suppress CH_4 emissions from this coastal plain wetland by as much as 85–93 %. Although increases in saltwater SO_4^{2-} loading to coastal wetlands may substantially reduce coastal plain wetland CH_4 emissions, enhanced N_2O emissions from high concentrations of NO_3^- in agricultural runoff may completely offset the reductions in CH_4. To predict large-scale changes in greenhouse emissions from coastal plain wetlands, future research should address the timing and spatial extent of both

saltwater incursion and agricultural runoff, as well as the greenhouse gas response to increasingly high concentrations of marine salts. As coastal plain wetland landscapes that make up the boundary between freshwater and saline ecosystems are progressively encroached upon by agricultural influences and saltwater incursion, we need to develop a predictive understanding of their likely trajectories of change, and the resulting feedbacks to climate change.

Acknowledgments We thank Steven Gougherty, Valerie Schoepfer, and Brooke Hassett for field and lab assistance, and Raven Bier for providing the first draft of Supplemental Fig. 1. Funding for this work was provided by NSF DEB 1216916.

References

Anderson CJ, Lockaby BG (2012) Seasonal patterns of river connectivity and saltwater intrusion in tidal forested wetlands. River Res Appl 28:814–826. doi:10.1002/rra.1489

APHA (1998) Standard method for examination of water and wastewater. American Public Health Association Publication, APHA, AWWA, WEF, Washington, DC

Ardón M, Morse JL, Doyle MW, Bernhardt ES (2010) The water quality consequences of restoring wetland hydrology to a large agricultural watershed in the Southeastern Coastal Plain. Ecosystems 13:1060–1078. doi:10.1007/s10021-010-9374-x

Ardón M, Morse J, Colman B, Bernhardt ES (2013) Drought-induced saltwater incursion leads to increased wetland nitrogen export. Glob Chang Biol 19:2976–2985. doi:10.1111/gcb.12287

Barendregt A, Whigham DF, Baldwin AH (2009) Preface. In: Barendregt A, Whigham D, Baldwin A (eds) Tidal freshwater wetlands. Backhuys Publishers, Leiden, pp 1–10

Bartlett KB, Bartlett DS, Harriss RC, Sebacher DI (1987) Methane emissions along a salt marsh salinity gradient. Biogeochemistry 4:183–202. doi:10.1007/BF02187365

Bloom AA, Palmer PI, Fraser A et al (2010) Large-scale controls of methanogenesis inferred from methane and gravity spaceborne data. Science 327:322–325. doi:10.1126/science.1175176

Brettar I, Rheinheimer G (1991) Denitrification in the central Baltic—evidence for H2S-oxidation as motor of denitrification at the oxic-anoxic interface. Mar Ecol Prog Ser 77:157–169

Brinson MM, Eckles SD (2011) US Department of Agriculture conservation program and practice effects on wetland ecosystem services: a synthesis. Ecol Appl 21(3):S116–S127

Burgin AJ, Hamilton SK, Jones SE, Lennon JT (2012) Denitrification by sulfur-oxidizing bacteria in a eutrophic lake. Aquat Microb Ecol 66:283–293

Capone DG, Kiene RP (1988) Comparison of microbial dynamics in marine and freshwater sediments: contrasts in anaerobic carbon catabolism. Limnol Oceanogr 33(4): 725–749

Carter LJ (1975) Agriculture: a new frontier in coastal North Carolina. Science 189:271–275. doi:10.1126/science.189.4199.271

Collins R, Jenkins A (1996) The impact of agricultural land use on stream chemistry in the middle hills of the Himalayas, Nepal. J Hydrol 185:137–150

Conrad R (1995) Methane emission from hypersaline microbial mats: lack of aerobic methane oxidation activity. FEMS Microbiol Ecol 16:297–305. doi:10.1016/0168-6496(95)00004-T

Corbett DR, Vance D, Letrick E et al (2007) Decadal-scale sediment dynamics and environmental change in the Albemarle Estuarine System, North Carolina. Estuar Coast Shelf Sci 71:771–729

Costanza R, d'Arge R, de Groot R et al (1997) The value of the world's ecosystem services and natural capital. Nature 387:253–260. doi:10.1038/387253a0

Costanza R, Perez-maqueo O, Martinez ML et al (2008) The value of coastal wetlands for hurricane protection. AMBIO 37(4):241–248

Dahl TE (1990) Wetlands losses in the United States 1780s to 1980s. Department of the Interior, Fish and Wildlife Service, Washington, DC

Day RH, Williams TM, Swarzenski CM (2007) Hydrology of tidal freshwater forested wetlands of the Southeastern United States. In: Conner WH, Doyle TW, Krauss KW (eds) Ecology of tidal freshwater forested wetlands of the southeastern United States. Springer, Dordrecht, pp 29–63

De Steven D, Gramling JM (2012) Diverse characteristics of wetlands restored under the Wetlands Reserve Program in the Southeastern United States. Wetlands 32:593–604. doi:10.1007/s13157-012-0303-y

Fogg P, Sangster J (2003) Chemicals in the atmosphere: solubility, sources, and reactivity. John Wiley, New York

Forster P, Ramaswamy V, Artaxo P et al (2007) Changes in atmospheric constituents and in radiative forcing. In: Solomon S, Qin D, Manning M, Chen Z, Marquis M, Averyt KB, Tignor M, Miller HL (eds) Climate change 2007: the physical science basis. Contribution of Working Group I to the Fourth Assessment Report of the Intergovernmental Panel on Climate Change. Cambridge University Press, Cambridge

Gauci V, Matthews E, Dise N et al (2004) Sulfur pollution suppression of the wetland methane source in the 20th and 21st centuries. Proc Natl Acad Sci USA 101:12583–12587. doi:10.1073/pnas.0404412101

Golterman HL, Clymo RS (eds) (1969) Methods for chemical analysis of sulphide in fresh waters, vol 8. Blackwell Scientific, Oxford

Heimlich RE, Wiebe KD, Claassen R, Gadsby D, House RM (1998) Wetlands and agriculture: private interests and public benefits. Agricultural economic report. USDA, Washington, DC

Hopfensperger KN, Burgin AJ, Schoepfer VA, Helton AM (2014) Impacts of saltwater incursion on plant communities, anaerobic metabolism, and resulting relationships in a restored freshwater wetland. Ecosystems. doi:10.1007/s10021-014-9760-x

Hudson F (2004) Standard operating procedure: sample preparation and calculations for dissolved gas analysis in water samples using a GC headspace equilibration technique. RSKSOP-175 US. EPA, Washington, DC

Hyer KE, Hornberger GM, Herman JS (2001) Processes controlling the episodic streamwater transport of atrazine and other agrichemicals in an agricultural watershed. J Hydrol 254:47–66

IPCC (2012) Summary for policymakers. In: Field CB, Barros V, Stocker TF, Qin D, Dokken DJ, Ebi KL, Mastrandrea MD, Mach KJ, Plattner GK, Allen SK, Tignor M, Midgley PM (eds) Managing the risks of extreme events and disasters to advance climate change adaptation. A special report of Working Groups I and II of the Intergovernmental Panel on Climate Change. Cambridge University Press, Cambridge

Joye SB, Hollibaugh JT (1995) Influence of sulfide inhibition of nitrification on nitrogen regeneration in sediments. Science 270:623–625. doi:10.1126/science.270.5236.623

Kozlowski TT (1997) Responses of woody plants to flooding and salinity. Tree Physiology Monograph No. 1. Heron Publishing, Victoria

Livingston GP, Hutchinson GL (1995) Enclosure-based measurement of trace-gas exchange: applications and sources of error. In: Matson PA, Harriss RC (eds) Biogenic trace gases: measuring emissions from soil and water. Blackwell Science, Cambridge, pp 14–51

Marton JM, Herbert ER, Craft CB (2012) Effects of salinity on denitrification and greenhouse gas production from laboratory-incubated tidal forest soils. Wetlands 32:347–357. doi:10.1007/s13157-012-0270-3

Matson A, Pennock D, Bedard-Haughn A (2009) Methane and nitrous oxide emissions from mature forest stands in the boreal forest, Saskatchewan, Canada. Forest Ecol Manag 258(7):1073–1083

Megonigal J, Hines M (2003) Anaerobic metabolism: linkages to trace gases and aerobic processes. In: Holland HD, Turekian KK (eds) Treatise on geochemistry, biogeochemistry, vol 8., pp 317–424

Morse JL, Ardón M, Bernhardt ES (2012) Greenhouse gas fluxes in southeastern US coastal plain wetlands under contrasting land uses. Ecol Appl 22:264–280. doi:10.1890/11-0527.1

Neubauer SC (2012) Ecosystem responses of a tidal freshwater marsh experiencing saltwater incursion and altered hydrology. Estuaries Coasts. doi:10.1007/s12237-011-9455-x

Nisbet EG, Dlugokencky EJ, Bousquet P (2014) Methane on the rise—again. Science 343:493–495. doi:10.1126/science.1247828

O'Driscoll MA (2012) The 1909 North Carolina drainage act and agricultural drainage effects in eastern North Carolina. N C Acad Sci 128:59–73

Oh NH, Raymond PA (2006) Contribution of agricultural liming to riverine bicarbonate export and CO_2 sequestration in the Ohio River basin. Glob Biogeochem Cycles 20:GB3012

Paerl HW, Bales JD, Ausley LW et al (2001) Ecosystem impacts of three sequential hurricanes (Dennis, Floyd, and Irene) on the United States' largest lagoonal estuary, Pamlico Sound, NC. PNAS 98(10):5655–5660

Poffenbarger HJ, Needelman BA, Megonigal JP (2011) Salinity influence on methane emissions from tidal marshes. Wetlands 31(5):831–842

R Core Team (2012) R: A language and environment for statistical computing. R Foundation for Statistical Computing, Vienna, Austria. http://www.R-project.org/

Roseberg RJ, Christensen NW, Jackson TL (1986) Chloride, soil solution osmotic potential, and soil-pH effects on nitrification. Soil Sci Soc Am J 50(4):941–945

Segers R (1998) Methane production and methane consumption: a review of processes underlying wetland methane fluxes. Biogeochemistry 41:23–51

Senga Y, Mochida K, Fukumori R et al (2006) N_2O accumulation in estuarine and coastal sediments: the influence of H_2S on dissimilatory nitrate reduction. Estuar Coast Shelf Sci 67:231–238. doi:10.1016/j.ecss.2005.11.021

Seo DC, Yu K, Delaune RD (2008) Influence of salinity level on sediment denitrification in a Louisiana estuary receiving diverted Mississippi River water. Arch Agron Soil Sci 54:249–257

Smith VH, Joye SB, Howarth RW (2006) Eutrophication of freshwater and marine systems. Limnol Oceanogr 51(1 part 2):351–355

Verhoeven JTA, Arheimer B, Yin C, Hefting M (2006) Regional and global concerns over wetlands and water quality. Trends Ecol Evol 21(2):96–103

Weston NB, Giblin A, Banta G et al (2010) The effects of varying salinity on ammonium exchange in estuarine sediments of the Parker River, Massachusetts. Estuaries Coasts 33:985–1003. doi:10.1007/s12237-010-9282-5

Weston NB, Vile MA, Neubauer SC, Velinsky DJ (2011) Accelerated microbial organic matter mineralization following salt-water intrusion into tidal freshwater marsh soils. Biogeochemistry 102:135–151. doi:10.1007/s10533-010-9427-4

Yates TT, Si BC, Farrell RE, Pennock DJ (2006) Probability distribution and spatial dependence of nitrous oxide emission: temporal change in hummocky terrain. Soil Sci Soc Am J 70(3):753–762

Zedler JB (2003) Wetlands at your service: reducing impacts of agriculture at the watershed scale. Front Ecol Environ 1:65–72. doi:10.1890/1540-9295(2003)001[0065:WAYSRI]2.0.CO;2